

A Near-Infrared AIE Probe for Super-Resolution Imaging and Nuclear Lipid Droplets Dynamic Study

Ming-Yu Wu,^{‡ab} Jong-Kai Leung,^{‡b} Chuen Kam,^b Tsu Yu Chou,^b Dong Wang,^c Shun Feng^a and Sijie Chen^{*b}

a School of Life Science and Engineering, Southwest Jiaotong University, Chengdu 610031, China.

b Ming Wai Lau Centre for Reparative Medicine, Karolinska Institutet, Hong Kong, China. E-mail: sijie.chen@ki.se.

c Center for AIE Research, College of Materials Science and Engineering, Shenzhen University, Shenzhen 518060, China.

Table of Contents

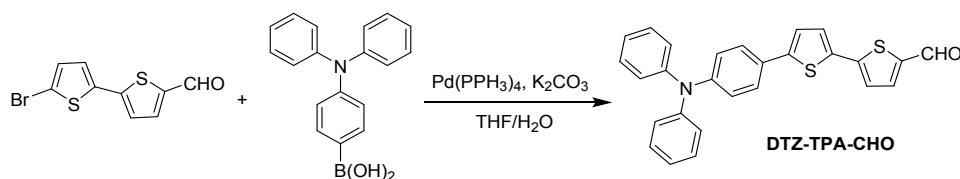
1. Experimental Procedures	S2
1.1 Materials and general instruments	S2
1.2 Synthesis and characterization of DTZ-TPA-DCN	S2
1.3 Cell culture.....	S3
1.4 CCK-8 assay for the determination of cell cytotoxicity and phototoxicity	S3
1.5 Fluorescence labeling	S4
1.6 Confocal laser scanning and super-resolution imaging	S4
2. Optical Properties of DTZ-TPA-DCN.....	S5
3. Cytotoxicity of DTZ-TPA-DCN.....	S5
4. Colocalization of DTZ-TPA-DCN and Commercial Fluorescent Probe for LDs	S6
5. Performance of DTZ-TPA-DCN in Fixed Cell Staining	S7
6. Super-Resolution Imaging of DTZ-TPA-DCN in HepG2 Cells	S8
7. Comparison of DTZ-TPA-DCN Performance between Confocal Imaging and Super-Resolution Imaging	S9
8. Z-stacked Images of nLDs with DTZ-TPA-DCN	S10
8. Nuclear Lipid Droplets Dynamic Study	S11
8. NMR and Mass Spectra	S15
9. Reference	S16

1. Experimental Procedures

1.1 Materials and general instruments

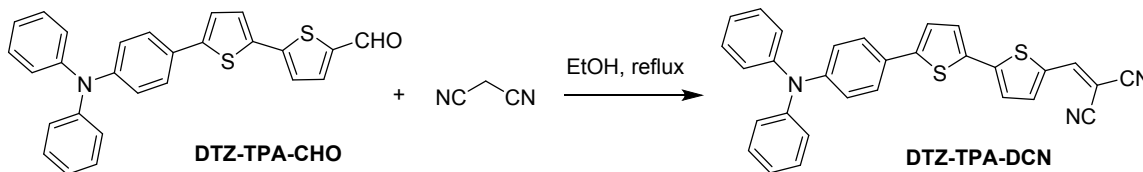
All chemical reagents were obtained from J&K Scientific and were used without further purification. Hoechst 33342 was available from Sigma-Aldrich. BODIPY™ 493/503 (4,4-difluoro-1,3,5,7,8-pentamethyl-4-bora-3a,4a-diaza-s-indacene) was purchased from Thermo Fisher Scientific. All the solvents for optical spectroscopic studies were HPLC or spectroscopic grade. Thin-layer chromatography analyses were performed on silica gel GF 254. Column chromatography purification was carried out on silica gel (200–300 mesh). NMR spectra were recorded using a Bruker AMX-400. Chemical shifts were given in ppm relative to the internal reference TMS or CDCl₃ as the internal standard. The following abbreviations were used in ¹H NMR: s = singlet; d = doublet; t = triplet; q = quartet; m = multiplet. High resolution mass spectra were recorded on a Bruker Daltonics Bio TOF mass spectrometer. Fluorescence spectra were obtained using a Horiba Duetta spectrofluorimeter with a 10 mm quartz cuvette. UV-Vis absorption spectra were recorded on a Hitachi PharmaSpec UV-1900 UV-Visible spectrophotometer. The average particle size of the samples was recorded on a Brookhaven Zeta Plus potential analyzer at 25 °C. The fluorescence distribution was monitored by the Zeiss LSM 880 confocal laser scanning microscope.

1.2 Synthesis and characterization of DTZ-TPA-DCN



DTZ-TPA-CHO was synthesised according to literature with further modification¹: 5'-bromo-[2,2'-bithiophene]-5-carbaldehyde (273 mg, 1 mmol), (4-(diphenylamino)phenyl)boronic acid (347 mg, 1.2 mmol), Pd(PPh₃)₄ (20 mg), and K₂CO₃ (1.38 g, 10 mmol) in 35 mL of THF/water (6:1, v/v) were refluxed overnight under nitrogen. After cooling to room temperature and removing the THF, the mixture was extracted with dichloromethane (DCM) for three times. The organic phase was collected, washed with saturated salt solution, and dried over anhydrous sodium sulfate. After solvent evaporation, the mixture was purified by silica gel column

chromatography using DCM/ Hex (2:1, v/v) as eluent to obtain 385 mg yellow solid (90.2% yield).



A solution of DTZ-TPA-CHO (87.5 mg, 0.2 mmol) and malononitrile (26.4 mg, 0.4 mmol) in dry ethanol (15 mL) was refluxed under nitrogen for 48 h. After the reaction mixture was cooled to ambient temperature, the solvent was evaporated under reduced pressure. The residue was purified by a silica gel column chromatography using Hex/DCM mixture (3:1, v/v) as eluent to give a dark red product (85 mg) in 87.5% yield. ¹H NMR (400 MHz, CDCl₃) δ: 7.67 (s, 1H), 7.55 (d, 1H, *J* = 3.2 Hz), 7.38 (dd, 2H, *J* = 1.6 Hz, *J* = 5.6 Hz), 7.32 (d, 1H, *J* = 3.2 Hz), 7.22 (t, 4H, *J* = 5.6 Hz), 7.19-7.18 (m, 2H), 7.14 (d, 1H, *J* = 2.8 Hz), 7.06 (d, 4H, *J* = 6.0 Hz), 7.02-6.98 (m, 5H). ¹³C NMR (100 MHz, CDCl₃) δ: 149.0, 148.8, 147.4, 146.9, 146.1, 139.3, 132.0, 128.4, 127.5, 125.7, 125.5, 123.9, 123.0, 122.6, 122.5, 121.8, 113.4, 112.6, 74.4. HRMS (ESI): *m/z* [M + H]⁺ calculated for C₃₀H₂₀N₃S₂: 486.1093; found 486.1078.

1.3 Cell culture

HepG2 cells were maintained in RPMI 1640 medium (Thermo Fisher Scientific) supplemented with 10% fetal bovine serum (FBS) (Thermo Fisher Scientific) and 100 units/mL of penicillin and 100 µg/mL of streptomycin in a 5% CO₂ humidified incubator at 37 °C. Once the cells reached 80%–90% confluence, they were dissociated into single cells with 0.05% Trypsin-EDTA (Thermo Fisher Scientific, USA) at 37 °C for 5 min and passaged at a ratio of 1:6–1:19 in a new cell culture dish. In corresponding experiments, HepG2 cells were further treated with 0.4 mM oleic acid (24 h) complexed with bovine serum albumin (Sigma-Aldrich), 5 µg/ml tunicamycin (Millipore Sigma, 12 h), 100 nM CP-346086 (Sigma-Aldrich, 12 h), or 10 µM diacylglycerol (Sigma-Aldrich, 12 h).

1.4 CCK-8 assay for the determination of cell cytotoxicity and phototoxicity

The cytotoxicity on HepG2 cells was determined by the standard WST-8 (2-(2-methoxy-4-nitrophenyl)-3-(4-nitrophenyl)-5-(2,4-disulfophenyl)-2H-tetrazolium, monosodium salt) (CCK-8) assay. HeLa cells were seeded at a density of 7 × 10³ cells per well in 96-well black microplates

with 100 μ L of culture medium and cultured overnight to reach 70–80% confluence. After that the medium was replaced with 100 μ L of fresh medium containing different concentrations of DTZ-TPA-DCN (0, 2.5, 5, 10, 15, 20 μ M) and DMSO was used as a vehicle control. After 24 h of incubation, 10 μ L of 12 mM CCK-8 stock solution (Sigma-Aldrich) mixed with 90 μ L of phosphate-buffered saline was added to each well for additional 4 h of incubation. The absorbance was measured at 450 nm using the SpectraMax M2 microplate reader (Molecular Devices). Cell viability (%) was calculated as: $(OD_{450} \text{ sample}/OD_{450} \text{ control}) \times 100\%$.

1.5 Fluorescence labeling

For cells fixation, cells were treated with 4% PFA for 15-20 minutes then rinsed by DPBS (Thermo Fisher Scientific) for three times. Live and fixed cells were stained with DTZ-TPA-DCN (1h), Hoechst 33342 (Sigma-Aldrich, 30 min), and/or BODIPY 493/503 (Thermo Fisher Scientific, 15 min) at 37°C. After the incubation, the staining solution was discarded, and cells were washed with DPBS for three times.

1.6 Confocal laser scanning and super-resolution imaging

Confocal imaging was performed using the Zeiss LSM 880 confocal laser scanning microscope equipped with a Plan-Apochromat 63 \times /1.4 NA oil objective lens, a photo-multiplier tube and a Gallium arsenide phosphide detector driven by the ZEN software (Carl Zeiss). The 514 nm laser and 550–650 nm emission filter were used for DTZ-TPA-DCN. The 405 nm laser and 460–490 nm emission filter were used for Hoechst 33342. The 488 nm laser and 510–540 nm emission filter were used for BODIPY 493/503. Digital images were captured and processed by ZEN software (ZEN 2.5 lite) in grayscale and pseudocolor. Super-resolution imaging was obtained using the N-SIM Super Resolution Microscope (Nikon), and the confocal image for comparison was obtained by the A1 HD25 confocal microscope (Nikon). Obtained images were then processed by NIS-Element imaging software (NIS-Elements AR, Nikon). To evaluate the photostability (Fig. 2D), we took 100 repetitive scans in the same area with 1 s interval time between two scans (Zeiss LSM 880 confocal laser scanning microscope, laser power: 2.47 μ W). The scanning of each frame took 3.78 s.

1.7 Data and Statistical Analysis

The Pearson Correlation Coefficient was obtained using the NIS-Element imaging software. For the statistical analysis, experiments were performed for at least three times, and data were presented as mean \pm standard deviation (SD). Statistical significance was determined by the Student's T-test, and * P value <0.05 was considered to be statistically significant.

2. Optical Properties of DTZ-TPA-DCN

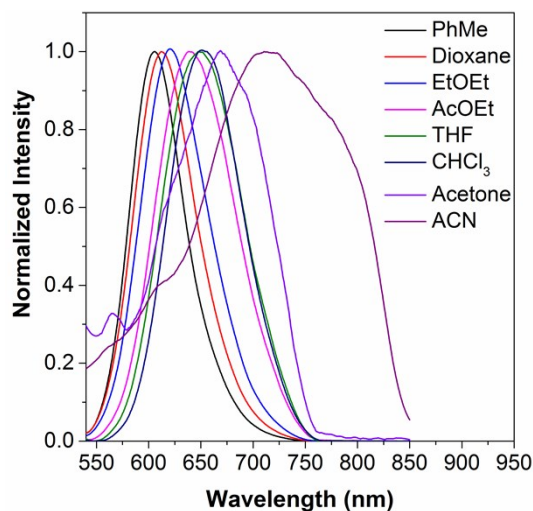


Fig. S1. PL spectra of DTZ-TPA-DCN in various solvents with different polarities.

3. Cytotoxicity of DTZ-TPA-DCN

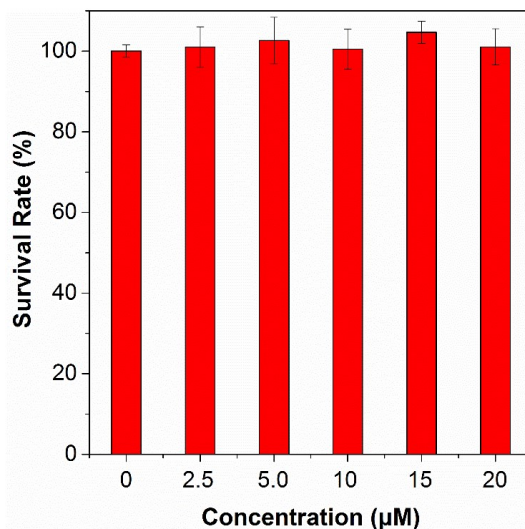


Fig. S2. Cell viability experiment of DTZ-TPA-DCN performed in HepG2 cells. The concentrations used in this experiment were 2.5, 5, 10, 15, 20 μM .

4. Colocalization of DTZ-TPA-DCN and Commercial Fluorescent Probe for LDs

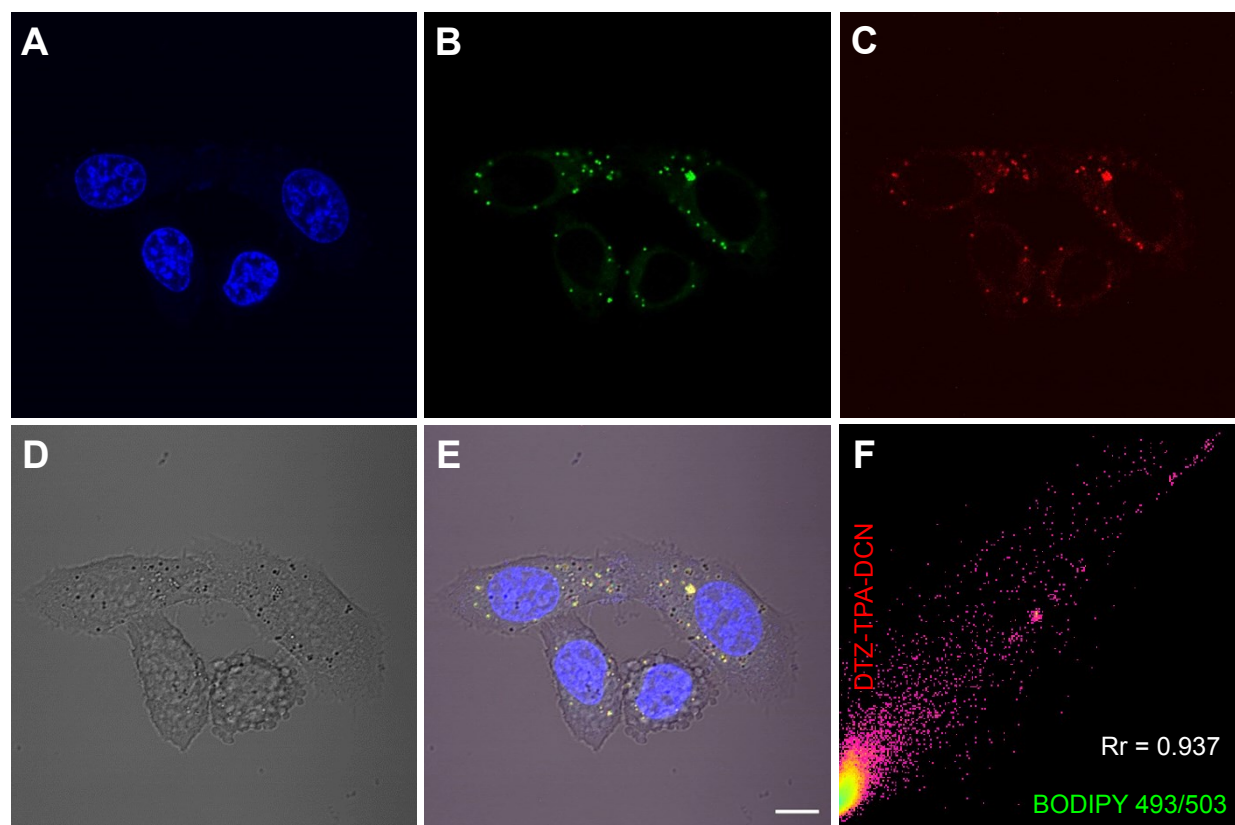


Fig. S3. LDs co-stained with commercial probes and **DTZ-TPA-DCN** in HepG2 cells. The fluorescence images were acquired by the confocal fluorescence microscope. (A) The nucleus of HepG2 cells were stained by Hoechst 33342 (blue). (B–C) LDs in the cytoplasm and nucleus were stained by BODIPY 493/503 (green) and **DTZ-TPA-DCN** (red). (D) Brightfield and (E) overlaid image of all four channels. Scale bar: 5 μm . (F) The scatter plot of the two channels with a Pearson correlation coefficient of 0.937.

5. Performance of DTZ-TPA-DCN in Fixed Cell Staining

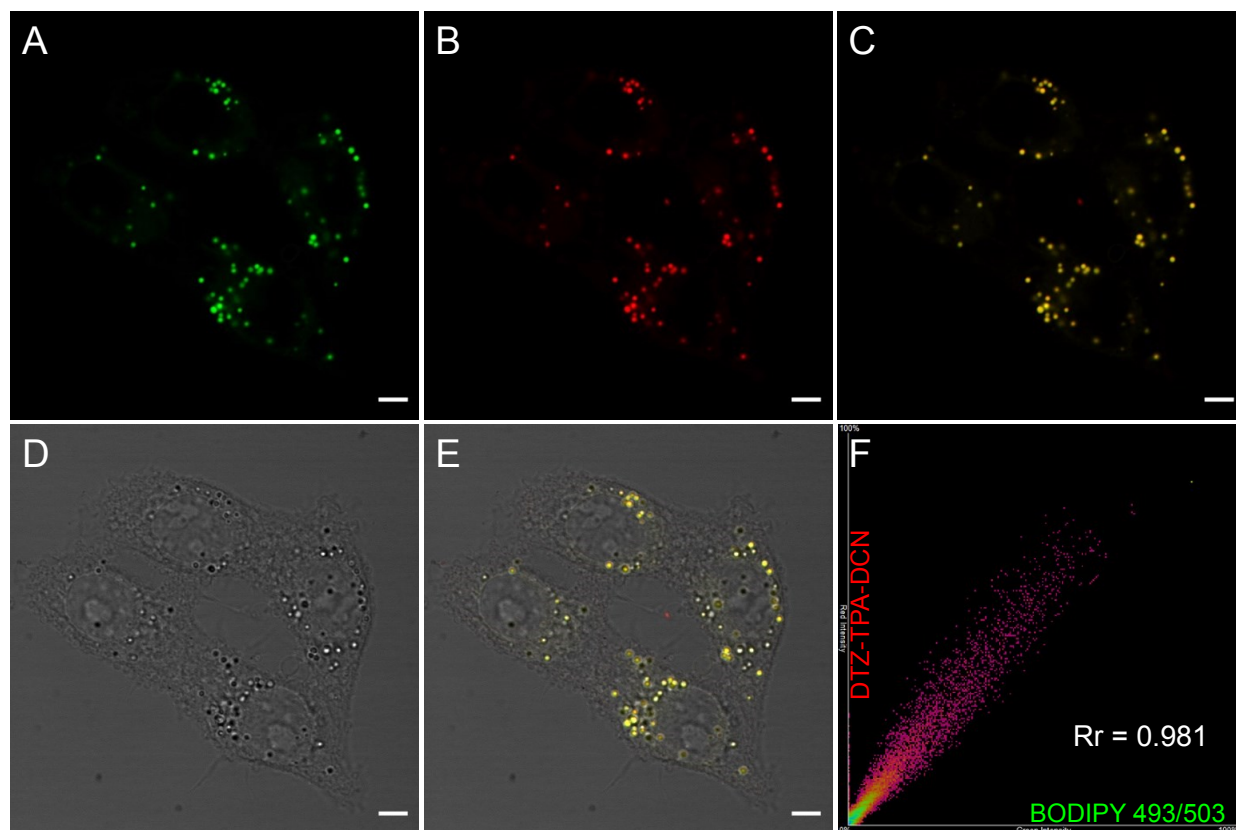


Fig. S4 Fixed HepG2's lipid droplets costained with commercial probes and **DTZ-TPA-DCN**. The fluorescent images were collected by the confocal fluorescent microscope. (A-B) nLDs were stained by BODIPY 493/503 (green) and **DTZ-TPA-DCN** (red). (C) Merged image of the green and red channel. (D) Brightfield of fixed HepG2 cells. (E) Merged image of all channels. (F) The scatter plot of the two channels with a Pearson correlation coefficient of 0.981. Scale bar: 10 μm .

6. Super-Resolution Imaging of DTZ-TPA-DCN in HepG2 Cells

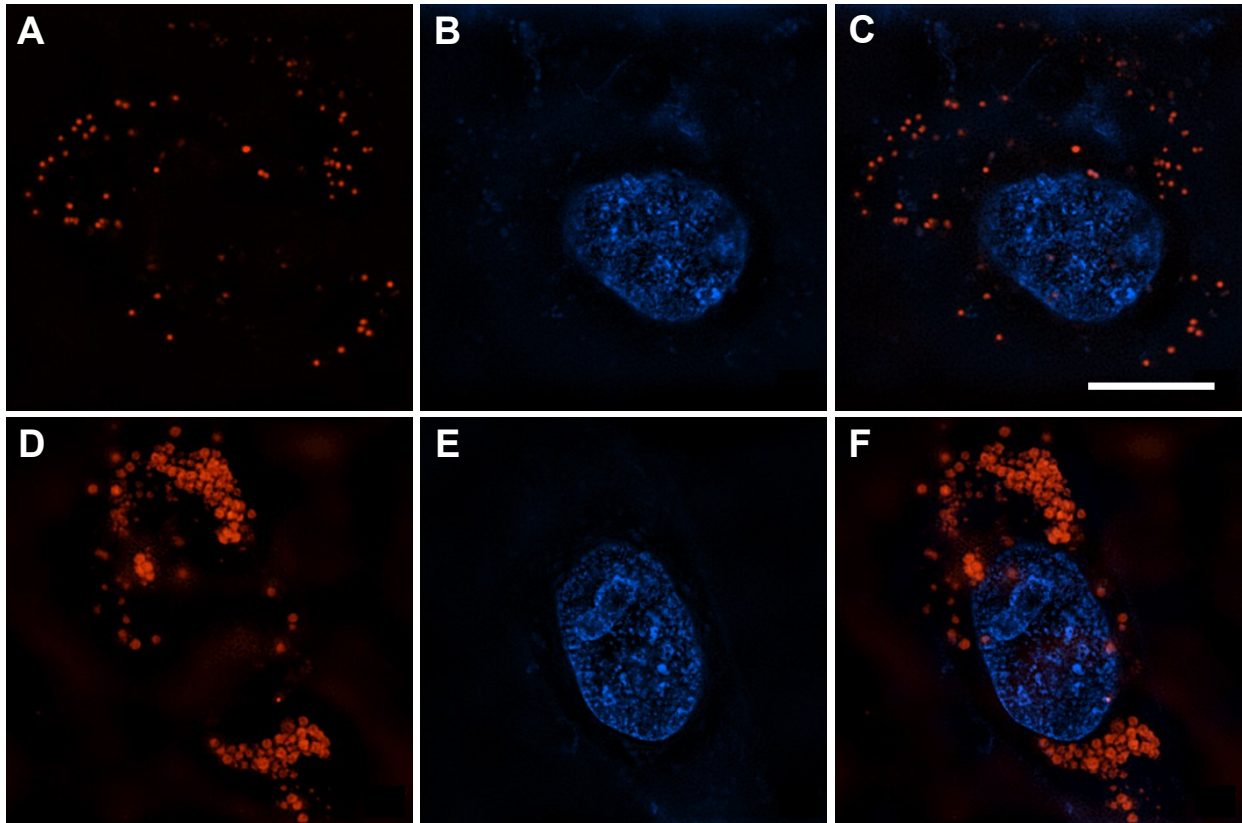


Fig. S5. Super-resolution imaging of LDs in live HepG2 cells. The fluorescence images were acquired by N-SIM. (A, D) LDs were stained by **DTZ-TPA-DCN** (red). (B, E) The nucleus of HepG2 cells were stained by Hoechst 33342 (blue). (C, F) Overlaid images of the two channels. (A–C) Images of HepG2 cells without OA treatment. (D–F) HepG2 cells treated with OA exhibited more LDs, and the size of LDs were larger. Scale bar: 10 μm .

7. Comparison of DTZ-TPA-DCN Performance between Confocal Imaging and Super-Resolution Imaging

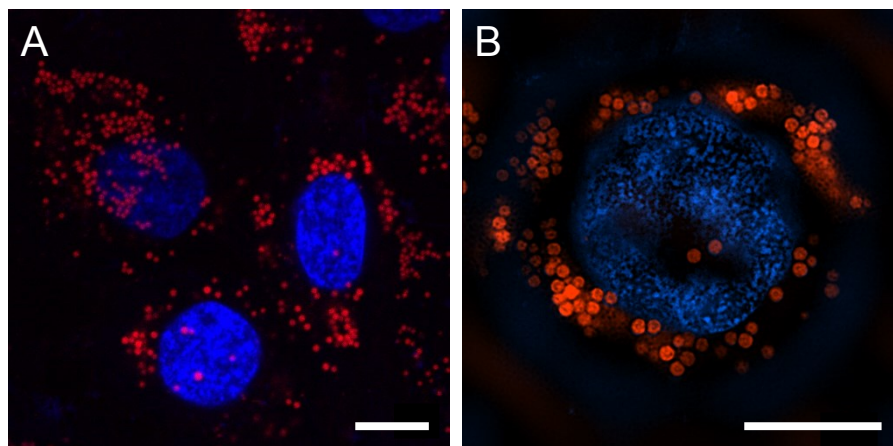


Fig. S6. Images of LDs obtained by different microscopes. The nucleus of live HepG2 cells were stained by Hoechst 33342 (blue), and LDs were stained by **DTZ-TPA-DCN** (red). (A) The image was acquired by the Zeiss LSM 880 confocal laser scanning microscope. (B) The image was acquired by the N-SIM Super Resolution Microscope. Scale bar: 10 μm .

8. Z-stacked Images of nLDs with DTZ-TPA-DCN

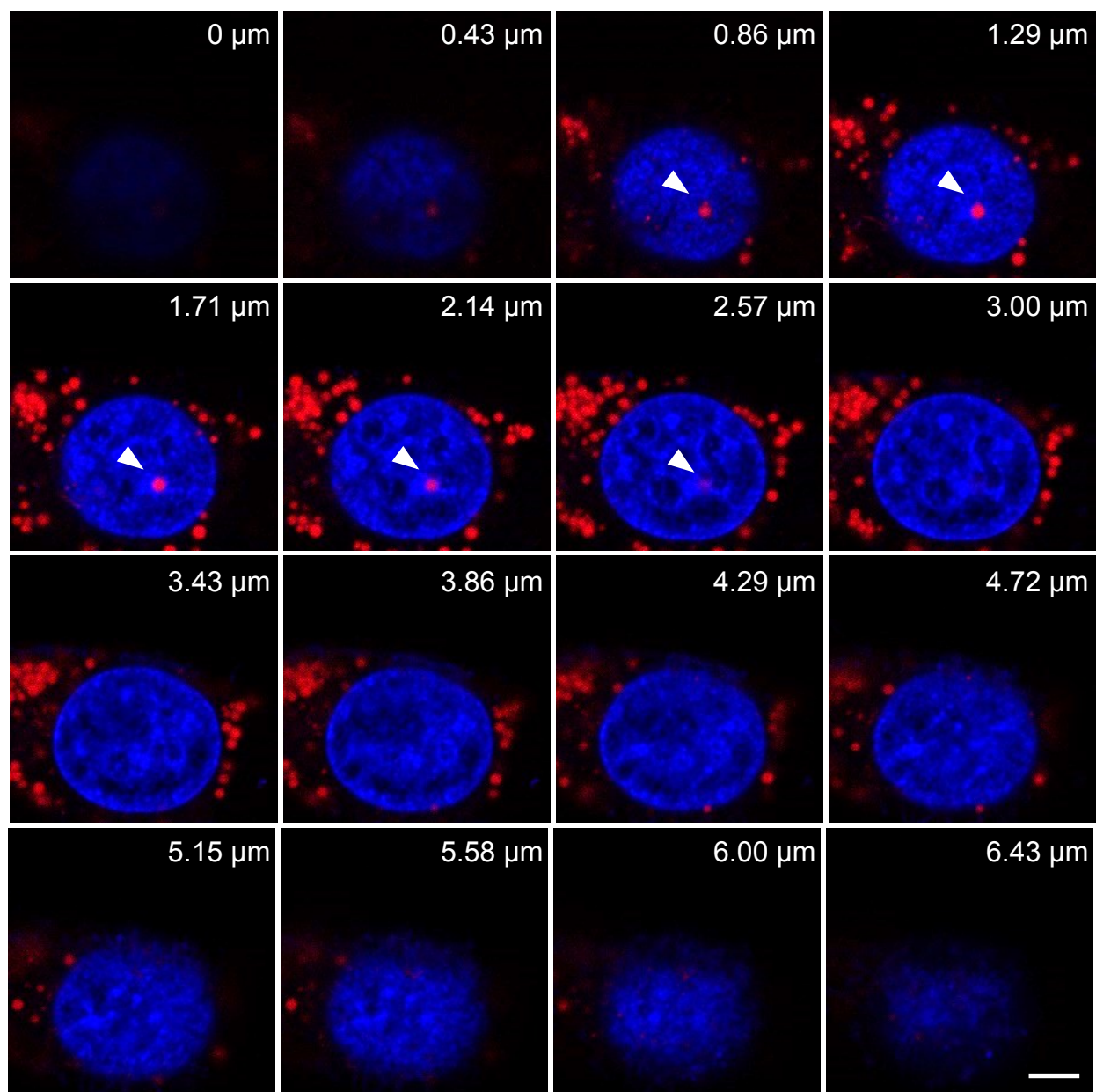


Fig. S7 Z-stacked images of Fig 4B. Scale bar: 10 μm .

8. Nuclear Lipid Droplets Dynamic Study

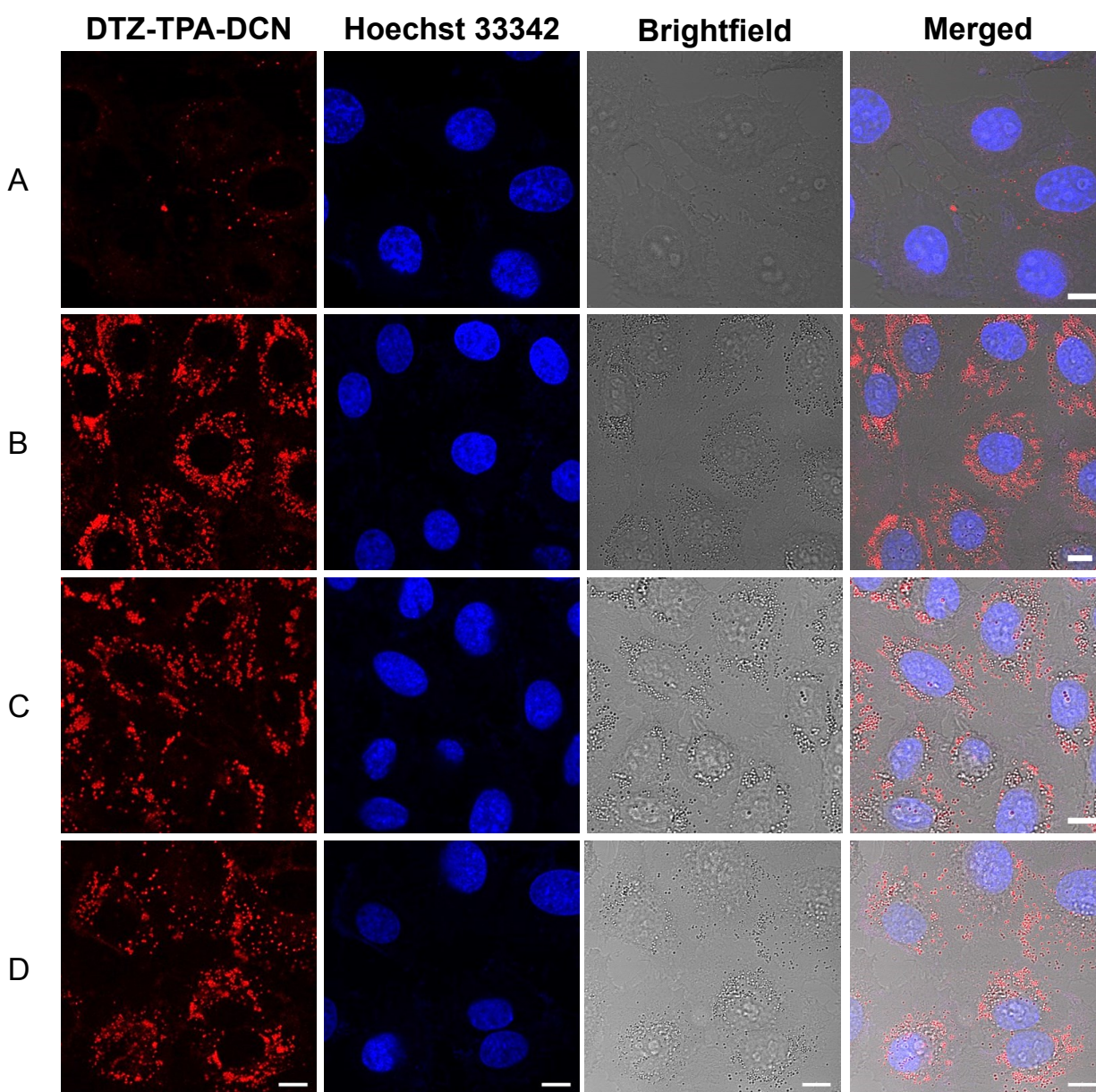


Fig. S8 Split images from Figure. 5. (A) Control group, HepG2 cells were treated with FBS. (B) HepG2 cells with OA treatment (C) HepG2 cells with OA + TM treatment (D) HepG2 cells with OA + TM + CP-346086 treatment. Scale bar: 10 μ m.

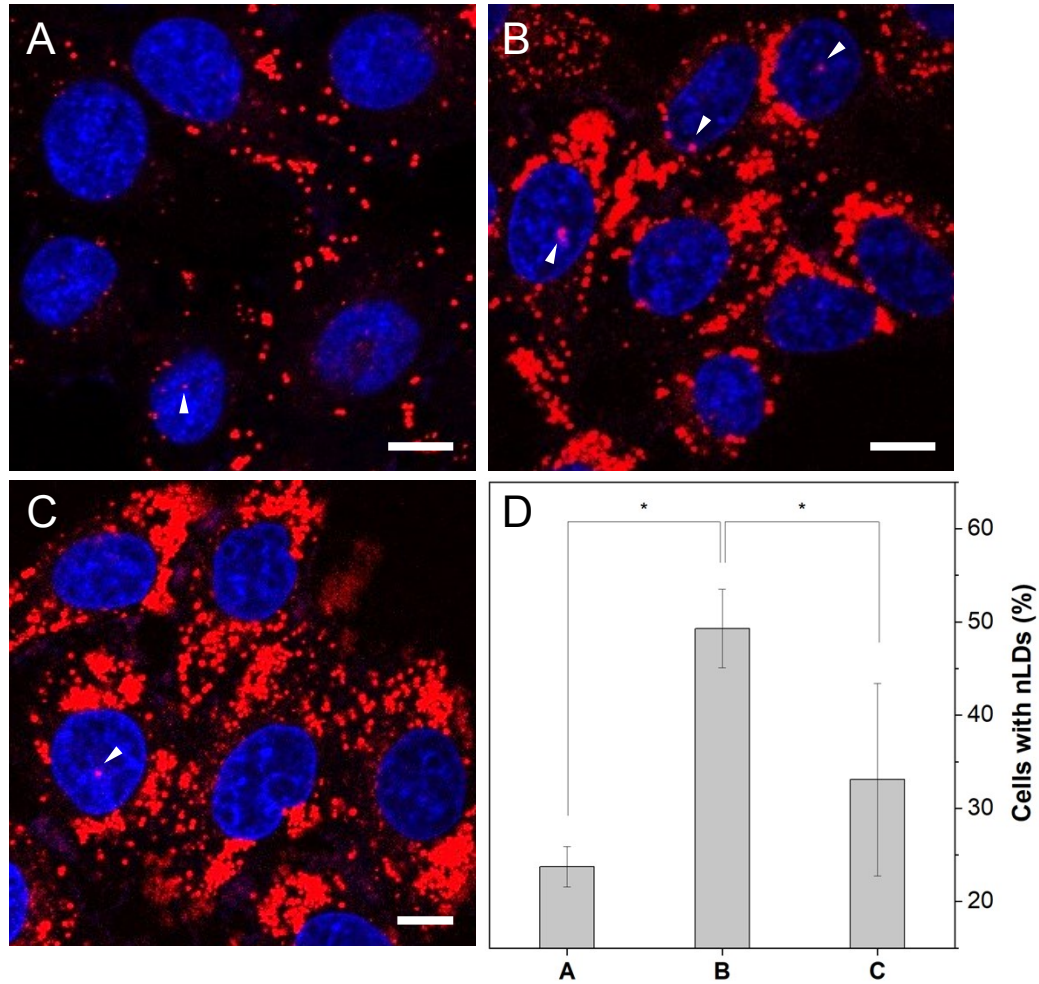


Fig. S9 DTZ-TPA-DCN in monitoring nLDs formation process. (A) HepG2 treated with FBS, the percentage of nLDs was about 23.7%. (B) HepG2 with OA treatment, and the percentage of nLDs increased to 49.3% (C) HepG2 with OA treatment and CP-346086 mM OA group, and percentage of nLDs decreased to 33.09%. Scale bar: 10 μ m. (D) Percentage of cells with nLDs in each group. Data are represented as mean \pm SEM from at least three independent experiments. (n=27/27/30, * P < 0.05)

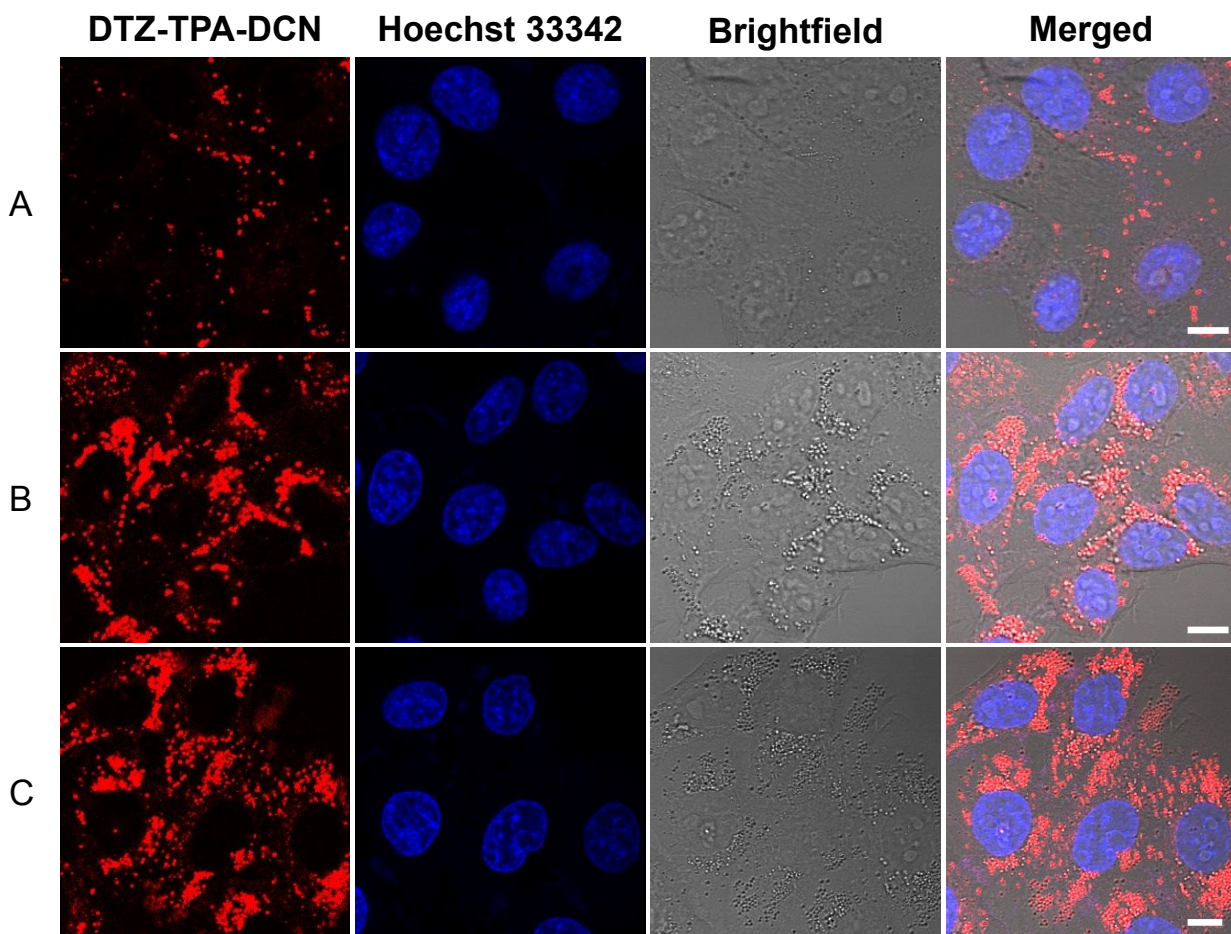


Fig. S10 Split images of Figure. S. (A) Control group, HepG2 cells were treated with FBS (B) HepG2 cells with OA treatment (C) HepG2 cells with OA and CP-346086 treatment. Scale bar: 10 μ m.

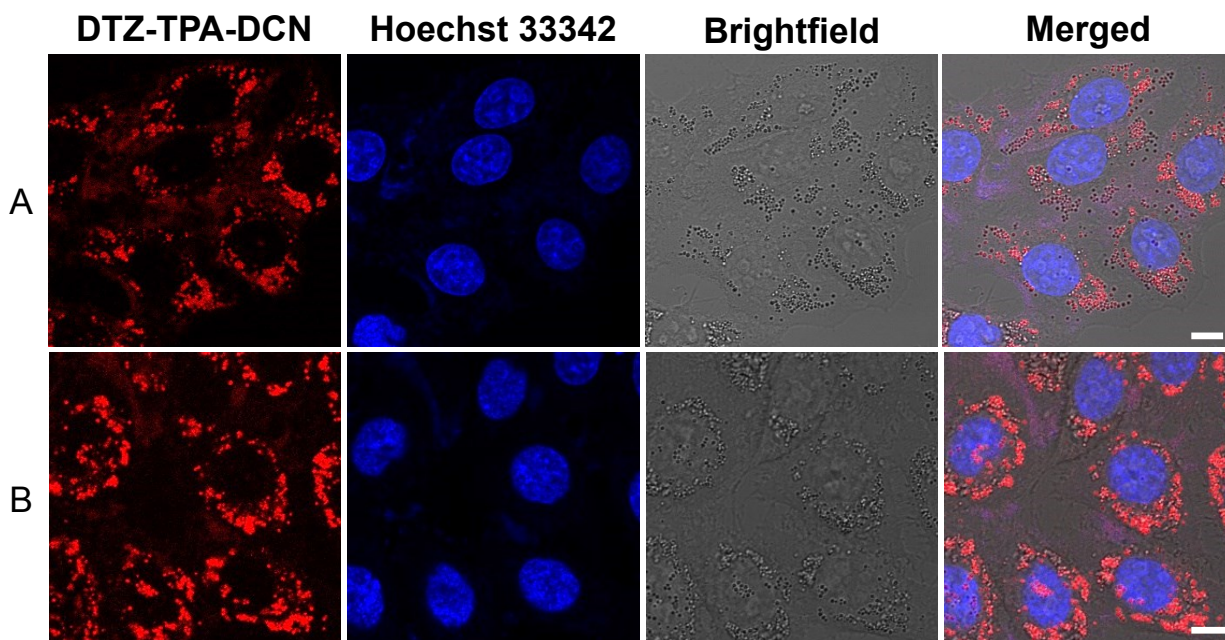
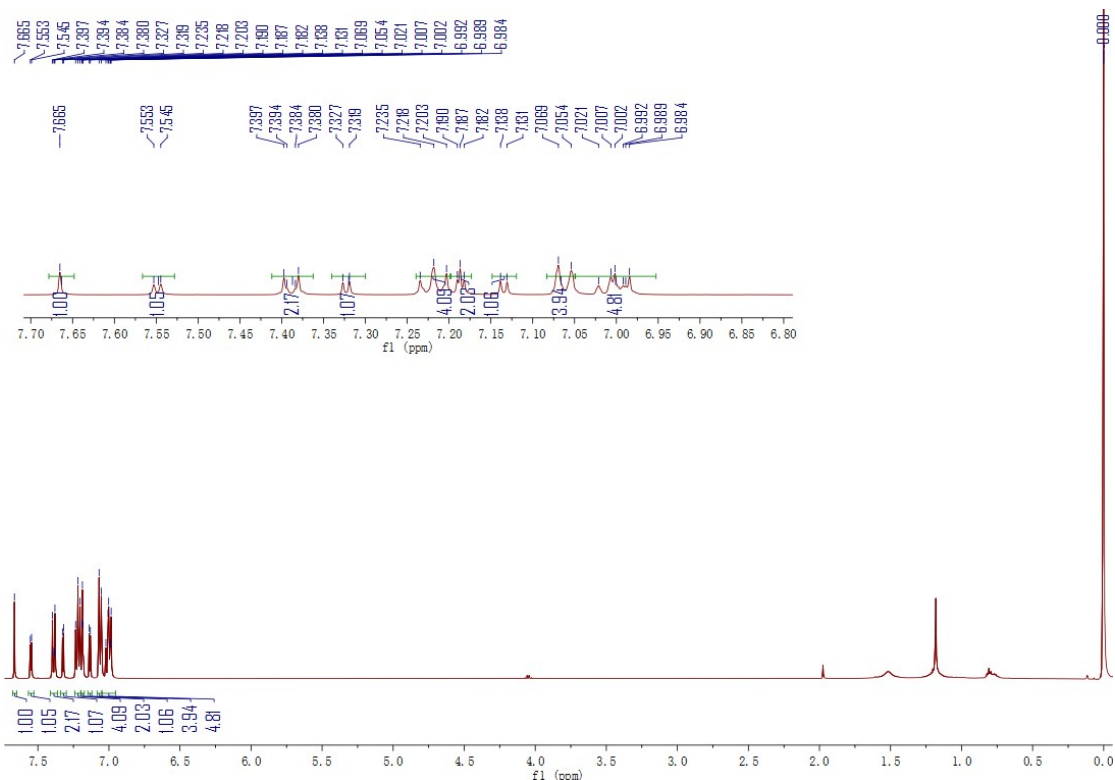
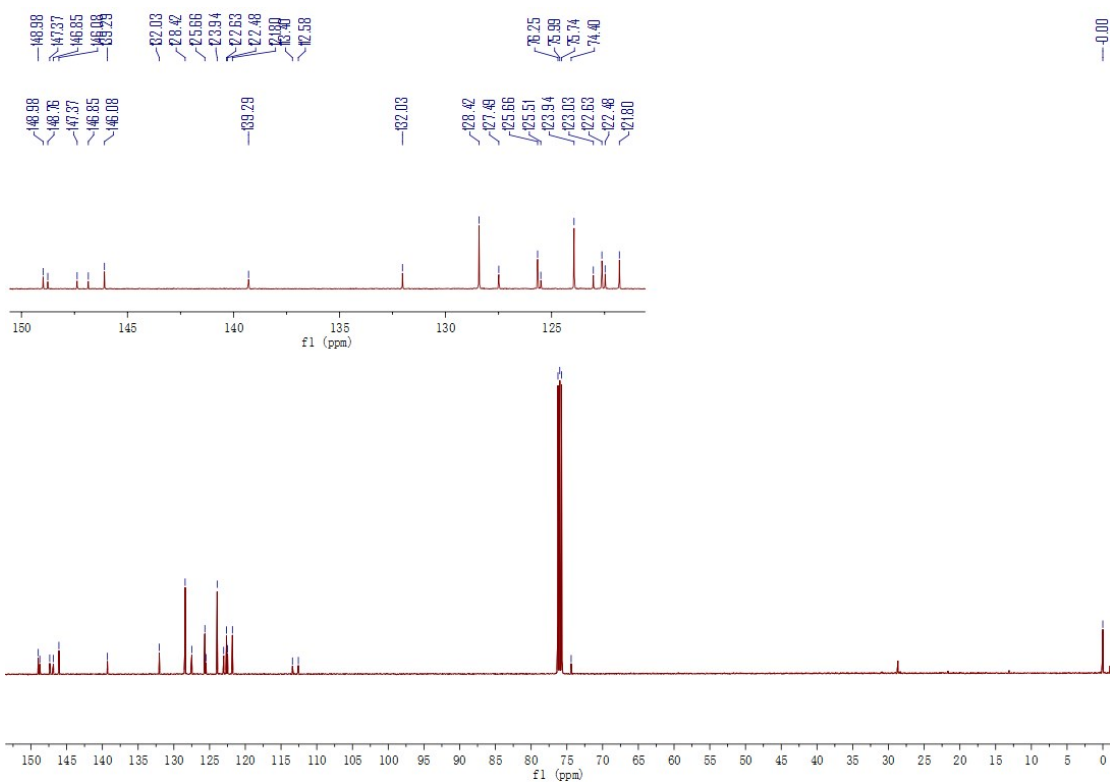


Fig. S11 Split images of Fig. 6. (A) Control group, HepG2 cells were treated with OA. (B) HepG2 cells with OA and DAG treatment. Scale bar: 10 μ m.

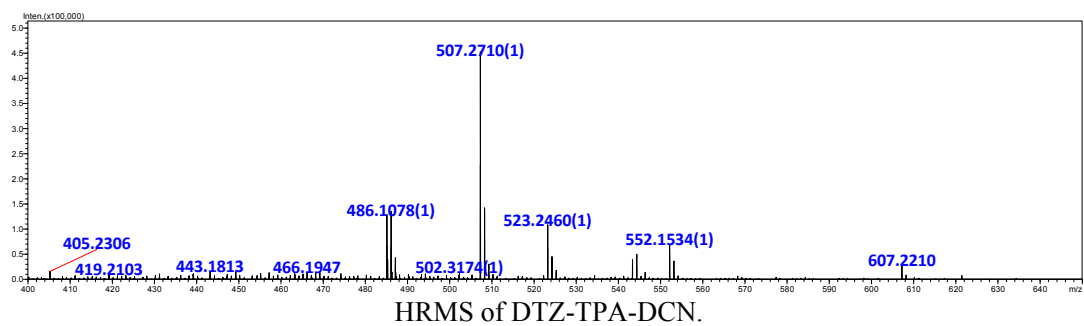
8. NMR and Mass Spectra



¹H NMR of DTZ-TPA-DCN in CDCl₃.



¹³C NMR of DTZ-TPA-DCN in CDCl₃.



9. Reference

- (1) H. E. Okda, S. E. Sayed, R. C. M. Ferreira, R. C. R. Gonçalves, S. P. G. Costa, M. M. M. Raposp, R. Martínez-Mañez and F. Sancenón, N,N-Diphenylanilino-heterocyclic aldehyde-based chemosensors for UV-vis/NIR and fluorescence Cu(II) detection, *New J. Chem.*, 2019, **43**, 7393-7402.